

DOI: 10.1002/zaac.202300208

Blue Emitting $\text{SrBe}_{1-x}\text{Si}_{2+x}\text{O}_{3-2x}\text{N}_{2+2x}:\text{Eu}^{2+}$ ($x \approx 0.1$)Tobias Gifftthaler,^[a] Marwin Dialer,^[a] Philipp Strobel,^[b] Peter J. Schmidt,^[b] and Wolfgang Schnick*^[a]

In the search for materials for high-efficiency lighting applications, the color-point tuning of phosphors for inorganic phosphor converted LEDs (pcLEDs) is of special interest. We expand the recently explored phosphor class of SiBeONs (oxonitridoberyllsilicates) by the synthesis and characterization of $\text{SrBe}_{1-x}\text{Si}_{2+x}\text{O}_{3-2x}\text{N}_{2+2x}:\text{Eu}^{2+}$. High temperature synthesis, starting from Sr_2N , BeO , SiO_2 and Si_3N_4 , yields the target phase as the main product. Upon doping with Eu^{2+} , the pale blue crystals

exhibit blue luminescence with emission at 456 nm and a full width at half maximum (*fwhm*) of 66 nm/3108 cm^{-1} . The structure is an ordered variant of the LaSi_3N_5 structure type and was elucidated by single-crystal X-ray diffraction data. The network in $\text{SrBe}_{1-x}\text{Si}_{2+x}\text{O}_{3-2x}\text{N}_{2+2x}:\text{Eu}^{2+}$ is highly condensed with a condensation degree of $\kappa = 0.6$ comprising corner-sharing $[\text{MX}_4]$ ($M = \text{Be}, \text{Si}; X = \text{O}, \text{N}$) tetrahedra, with mixed occupancies on both the ligand and central metal sites.

Introduction

As part of environmental efforts to save energy, solid-state lighting using phosphor-converted LEDs (pcLEDs) can contribute to a more energy-efficient future. In white emitting pcLEDs, ultraviolet (UV) or blue light emitted from a semiconductor chip is partially converted by ceramic phosphors to reproduce the spectral power distribution of natural white light in the visible spectral range. Hereby, the chemical tunability of applied phosphors is essential to achieve the desired emission. The luminescence of widely used aluminates and silicates, as well as their respective nitride equivalents, is conventionally tuned by substitution of the cations on the doped site. Industrially, this is applied in the red spectral region by emission optimization in $\text{AE}_2\text{Si}_5\text{N}_8:\text{Eu}^{2+}$ ($\text{AE} = \text{Ca}, \text{Sr}, \text{Ba}$) or $\text{Ca}_{1-x}\text{Sr}_x\text{AlSiN}_3:\text{Eu}^{2+}$ and in the green spectral region in $\text{RE}_{3-y}\text{Al}_{5-y}\text{Ga}_y\text{O}_{12}:\text{Ce}_x$.^[1–5]

As shown by the substitution of Si^{4+} by Al^{3+} or Li^+ , elemental substitutions at the network-building positions can also alter the emission of doped phosphors. In this case, charge neutrality is maintained by O/N/F substitution on the anion

sites, which changes the coordination environment of the emitter.^[6–7] Due to the nephelauxetic effect and crystal field splitting this leads to a change in emission wavelengths. Based on the comparable sizes of Be^{2+} and Si^{4+} cations (0.27 Å and 0.26 Å respectively, in tetrahedral coordination), beryllates in general are closely related to silicates and their respective nitride derivatives.^[8–12] Hence, replacing Al/Li/Si by Be can potentially be used as a third substitution pathway to target selected spectral regions more efficiently without altering the formal anionic composition.

An established cyan emitting phosphor is $\text{SrSiAl}_2\text{O}_3\text{N}_2:\text{Eu}^{2+}$, which has an emission maximum at ~487 nm with an *fwhm* greater than 85 nm, while spectral properties depend on the dopant concentration.^[13–15]

In this context, we report here on the derived, blue emitting phosphor $\text{SrBe}_{1-x}\text{Si}_{2+x}\text{O}_{3-2x}\text{N}_{2+2x}:\text{Eu}^{2+}$ (SBS).

Results and Discussion

High temperature synthesis of $\text{SrBe}_{1-x}\text{Si}_{2+x}\text{O}_{3-2x}\text{N}_{2+2x}:\text{Eu}^{2+}$ starting from Sr_2N , BeO , SiO_2 , Si_3N_4 and EuF_3 yielded an air- and moisture-insensitive pale blue powder. Powder X-ray diffraction (PXRD) experiments confirmed SBS as the main product phase (> 80 wt%) with SrBeSiO_4 , Sr_2SiO_4 and BeSiN_2 as minor side-products (see Figure S2). SBS crystallizes in the orthorhombic space group $P2_12_12_1$ (no. 19) with cell parameters $a = 4.7671(2)$, $b = 7.7683(2)$ and $c = 10.9364(3)$ Å and is an ordered variant of the LaSi_3N_5 structure type.^[16] The chemical composition of the target phase was confirmed by EDS (averaged over seven data points; $\text{Sr}_{1.0}\text{BeSi}_{2.8(2)}\text{O}_{3.3(1)}\text{N}_{2.3(3)}$; see table S1). Details of the crystal structure and product phase determination are given in the Supporting Information (tables S2–S5).

As shown in Figure 1, in SBS O and N coordinate Be and Si in corner sharing tetrahedra. This results in a highly condensed network with a degree of condensation $\kappa = 0.6$. Sr is (8 + 2)-fold coordinated by O and N in a distorted double capped square antiprism (Johnson polyhedron 17). Hereby, N sites are fully

[a] T. Gifftthaler, M. Dialer, Prof. Dr. W. Schnick
Department of Chemistry
University of Munich
Butenandtstraße 5–13 (D)
81377 Munich, Germany
E-mail: wolfgang.schnick@uni-muenchen.de

[b] Dr. P. Strobel, Dr. P. J. Schmidt
Lumileds Germany GmbH
Lumileds Phosphor Center Aachen
Philipsstraße 8
52068 Aachen, Germany

Supporting information for this article is available on the WWW under <https://doi.org/10.1002/zaac.202300208>

© 2023 The Authors. Zeitschrift für anorganische und allgemeine Chemie published by Wiley-VCH GmbH. This is an open access article under the terms of the Creative Commons Attribution Non-Commercial NoDerivs License, which permits use and distribution in any medium, provided the original work is properly cited, the use is non-commercial and no modifications or adaptations are made.

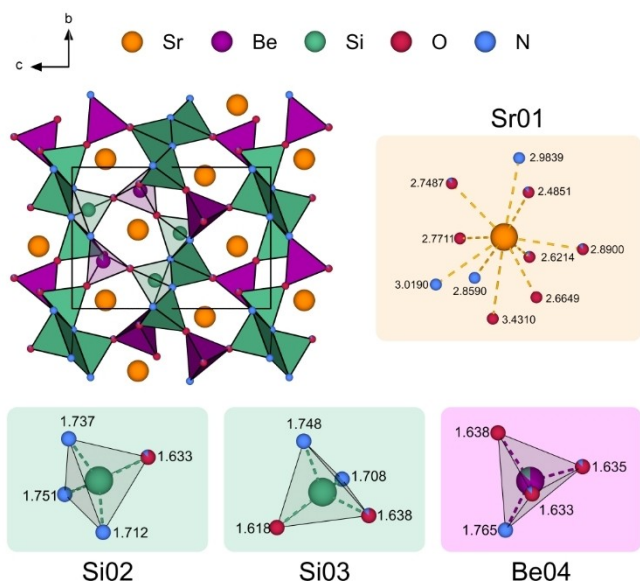


Figure 1. Structure of $\text{SrBe}_{1-x}\text{Si}_{2+x}\text{O}_{3-2x}\text{N}_{2+2x}:\text{Eu}^{2+}$. Sr orange, Be and $[\text{BeO}_3\text{N}]$ tetrahedra purple, Si and $[\text{SiO}_3\text{N}_2]$ tetrahedra green, O red, N blue; crystal structure projection along $[100]$; corner-sharing tetrahedra connected *via* O/N; coordination environments of the cations by O and N with atomic distances given in Å.

occupied, whereas two of three O sites are occupied by both O and N. The O sites and those with mixed occupancy can be identified by significantly shorter interatomic distances compared to the N sites in $[\text{MX}_4]$ ($M=\text{Be}$, Si $X=\text{N}$, O) tetrahedra. Charge neutrality is maintained, by a mixed occupation of the single Be site by Be and Si. Both Si sites are fully occupied. Tetrahedra form *fünfer-rings* with channels along $[100]$.^[17]

BVS and CHARDI calculations corroborate the proposed structure model and the assignment of mixed occupancies (see table S6).^[18–20]

Upon doping with Eu^{2+} and excitation with radiation wavelengths shorter than 400 nm, the target phase exhibits blue luminescence. Single crystal luminescence experiments showed a maximum emission at 456 nm and *fwhm* of 66 nm/ 3108 cm^{-1} (Figure 2). Compared to the structurally closely related $\text{SrSiAl}_2\text{O}_3\text{N}_2:\text{Eu}^{2+}$, SBS emits a narrower emission spectrum at shorter wavelengths. The slightly changed emission properties are likely due to a change in the orientation of Eu^{2+} $5d$ orbitals relative to their coordination sphere. The shorter average distances in SBS to the ligands and the smaller coordination polyhedron with respect to $\text{SrSiAl}_2\text{O}_3\text{N}_2:\text{Eu}^{2+}$ are typically not expected to result in shorter emission wavelengths.^[21] A similar anomaly has been observed in $\text{Sr}_{1-x}\text{Ba}_x\text{SiAl}_2\text{O}_3\text{N}_2:\text{Eu}^{2+}$, where chemical pressure of the second and third coordination sphere was used as an explanation.^[15] The difference is, that in SBS the coordination sphere increases compared to the respective reference and therefore other mechanisms must determine the emission. Hence, theoretical calculations of the crystal fields and excited states of Eu^{2+} ($4f^65d^1$) are necessary for further clarification.^[22]

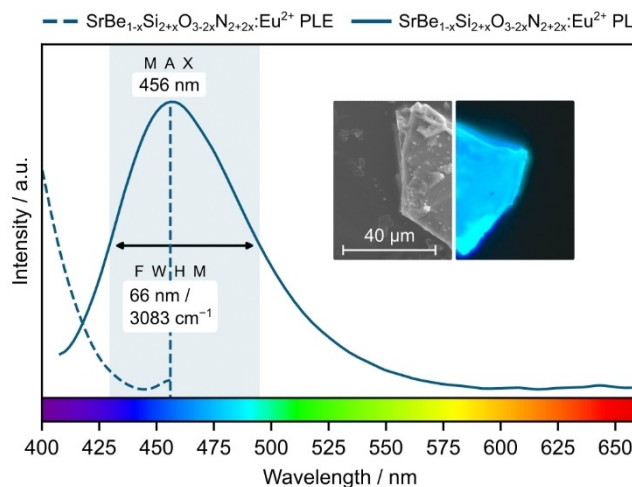


Figure 2. Luminescence spectrum of $\text{SrBe}_{1-x}\text{Si}_{2+x}\text{O}_{3-2x}\text{N}_{2+2x}:\text{Eu}^{2+}$. The excitation (blue dashed line) and emission of SBS under UV irradiation (blue line) with an emission maximum at 456 nm and a *fwhm* of 66 nm; selected particle of SBS in an optical and a scanning electron microscope.

The system $\text{SrSiAl}_2\text{O}_3\text{N}_2:\text{Eu}^{2+}/\text{SrBe}_{1-x}\text{Si}_{2+x}\text{O}_{3-2x}\text{N}_{2+2x}:\text{Eu}^{2+}$ can be an example of color point tuning of phosphors by Be substitution. However, due to the presence of minor phases and the use of toxic BeO as a precursor, industrial application of SBS is currently not a main focus. Instead, the route of using beryllium as an additional or substituting network building cation proves promising to enable activator sites in next generation luminescent materials with further optimized performance.

Conclusion and Outlook

The luminescent properties of $\text{SrBe}_{1-x}\text{Si}_{2+x}\text{O}_{3-2x}\text{N}_{2+2x}:\text{Eu}^{2+}$ illustrate the potential of SiBeONs for application as phosphor materials. It is shown that substitution of Be^{2+} for the known network-building cations Al^{3+} and Si^{4+} enables comparatively narrow-band emission. For further investigations, phase pure samples can be beneficial to determine quantum efficiencies as well as electronic properties like the band structure and gap. For further elucidation of mixed occupations, neutron scattering experiments could provide new insights.

SiBeONs in general can help to achieve desired emission characteristics in future phosphor applications, especially those containing low quantities of beryllium.

Experimental Section

Safety Precautions. BeO is characterized as toxic and was therefore exclusively handled in closed systems, under Schlenk conditions or inside a glovebox.^[23–24] For safety precautions the product was also handled under closed conditions, although, chemically stable multinary beryllates as the mineral beryl are not known to be harmful.

Synthesis. The starting materials Sr₂N (synthesized from Sr, *Sigma Aldrich*, 99.99%) BeO (*Alfa Aesar*, 99.95%), SiO₂ (*Acros Organics*, 60 A) and Si₃N₄ (*UBE*, SNA-00) were ground in a tungsten carbide mortar inside a glovebox (Unilab, *MBraun*, Garching; O₂ < 0.1 ppm, H₂O < 0.1 ppm) together with EuF₃ (*Sigma-Aldrich*, 99.99%) for luminescence experiments and transferred to a W crucible. Reactions were carried out in a radio frequency furnace (TIG 10/100; Hüttinger Elektronik Freiburg, Germany) under dried N₂ atmosphere. For the reaction the crucible was heated to 1600 °C in 30 minutes, the temperature was held for further 30 minutes, cooled down in 30 minutes to 600 °C and then quenched to room temperature by turning off the heating.

Single-Crystal X-ray diffraction. Data of micromount fixed single crystals of SrBe_{1-x}Si_{2+x}O_{3-2x}N_{2+2x}:Eu²⁺ were collected on a Bruker D8 Venture rotary anode diffractometer with Mo-K α radiation ($\lambda = 0.71073$ Å), that was focused with a Goebel mirror. The collected data was integrated and absorption corrected with APEX3.^[25] Structures were solved by direct methods with SHELXS and refined with SHELXL, applying the full-matrix least square method.^[26–27]

Powder X-ray diffraction. Powder samples were ground in a tungsten carbide mortar and sealed in glass capillaries (*Hilgenberg*, $d = 0.5$ mm). Measurements were carried out on a rotary head STOE STADI P diffractometer (Cu-K α radiation, Ge(111) monochromator, Mythen 1k detector) with modified Debye-Scherrer geometry. The TOPAS 6 software package was used for Rietveld refinement and determining of the given phase composition.^[28]

Elemental analysis. To determine the elemental composition of SrBe_{1-x}Si_{2+x}O_{3-2x}N_{2+2x}:Eu²⁺, energy dispersive X-ray spectroscopy (EDS) on a Dualbeam Helios Nanolab G3 UC scanning electron microscope (SEM, FEI) with X-Max 80 SDD detector (Oxford Instruments) was applied. Data of a selected particle were collected at an acceleration voltage of 25 kV.

Luminescence. Luminescence data of selected particles and single crystals were obtained on an Olympus BX51 microscope with a HORIBA Fluoromax4 spectrofluorimeter system attached. Particle and single crystal images were taken on a ZEISS AXIO imager M1 m microscope.

Acknowledgements

The authors thank Dr. Peter Mayer and Reinhard Pritzl for collecting single-crystal data as well as Christian Minke (all at Department of Chemistry, LMU Munich) for EDS measurements. Open Access funding enabled and organized by Projekt DEAL.

Conflict of Interest

The authors declare no conflict of interest.

Data Availability Statement

The data that support the findings of this study are available in the supplementary material of this article.

Keywords: Beryllium · Luminescence · Solid-state structures · Silicates · Nitrides

- [1] O. M. ten Kate, Z. Zhang, P. Dorenbos, H. T. Hintzen, E. van der Kolk, *J. Solid State Chem.* **2013**, *197*, 209–217.
- [2] T. Schlieper, W. Milius, W. Schnick, *Z. Anorg. Allg. Chem.* **1995**, *621*, 1380–1384.
- [3] H. Watanabe, N. Kijima, *J. Alloys Compd.* **2009**, *475*, 434–439.
- [4] J. M. Ogieglo, A. Katelnikovas, A. Zych, T. Justel, A. Meijerink, C. R. Ronda, *J. Phys. Chem. A* **2013**, *117*, 2479–2484.
- [5] D. Nakauchi, Y. Yoshida, N. Kawaguchi, T. Yanagida, *J. Mater. Sci. Mater. Electron.* **2019**, *30*, 14085–14090.
- [6] P. Pust, V. Weiler, C. Hecht, A. Tucks, A. S. Wochnik, A. K. Henss, D. Wiechert, C. Scheu, P. J. Schmidt, W. Schnick, *Nat. Mater.* **2014**, *13*, 891–896.
- [7] G. J. Hoerder, M. Seibald, D. Baumann, T. Schröder, S. Peschke, P. C. Schmid, T. Tyborski, P. Pust, I. Stoll, M. Bergler, C. Patzig, S. Reissaus, M. Krause, L. Berthold, T. Hoche, D. Johrendt, H. Huppertz, *Nat. Commun.* **2019**, *10*, 1824.
- [8] L. Eisenburger, O. Oeckler, W. Schnick, *Chem. Eur. J.* **2021**, *27*, 4461–4465.
- [9] S. Merlino, C. Biagioni, E. Bonaccorsi, N. V. Chukanov, I. V. Pekov, S. V. Krivovichev, V. N. Yakovenchuk, T. Armbruster, *Mineral. Mag.* **2018**, *79*, 145–155.
- [10] L. A. Harris, H. L. Yakei, *Acta Crystallogr. Sect. B* **1969**, *25*, 1647–1651.
- [11] P. Strobel, V. Weiler, P. J. Schmidt, W. Schnick, *Chem. Eur. J.* **2018**, *24*, 7243–7249.
- [12] N. Krishna Rao, T. Sreenivas, *Miner. Process. Extr. Metall. Rev.* **1994**, *13*, 19–42.
- [13] R. Lauterbach, W. Schnick, *Z. Anorg. Allg. Chem.* **1998**, *624*, 1154–1158.
- [14] X. Wang, Z. Zhao, Q. Wu, Y. Li, C. Wang, A. Mao, Y. Wang, *Dalton Trans.* **2015**, *44*, 11057–11066.
- [15] W.-Y. Huang, F. Yoshimura, K. Ueda, Y. Shimomura, H.-S. Sheu, T.-S. Chan, C.-Y. Chiang, W. Zhou, R.-S. Liu, *Chem. Mater.* **2014**, *26*, 2075–2085.
- [16] Z. Inoue, M. Mitomo, N. li, *J. Mater. Sci.* **1980**, *15*, 2915–2920.
- [17] F. Liebau, *Structural Chemistry of Silicates*, Springer, Berlin, Heidelberg, **1985**. The term “*fünfer ring*”, as defined by Liebau, describes a ring of five tetrahedra and is derived from the german word *fünf* – five.
- [18] N. E. Brese, M. O’Keeffe, *Acta Crystallogr. Sect. B* **1991**, *47*, 192–197.
- [19] I. D. Brown, D. Altermatt, *Acta Crystallogr. Sect. B* **1985**, *41*, 244–247.
- [20] R. Hoppe, S. Voigt, H. Glaum, J. Kissel, H. P. Müller, K. Bernet, *J. Less-Common Met.* **1989**, *156*, 105–122.
- [21] M.-H. Fang, C. O. M. Mariano, P.-Y. Chen, S.-F. Hu, R.-S. Liu, *Chem. Mater.* **2020**, *32*, 1748–1759.
- [22] R. Shafei, D. Maganas, P. J. Strobel, P. J. Schmidt, W. Schnick, F. Neese, *J. Am. Chem. Soc.* **2022**, *144*, 8038–8053.
- [23] O. Kumberger, H. Schmidbaur, *Chem. Unserer Zeit* **1993**, *27*, 310–316.
- [24] D. Naglav, M. R. Buchner, G. Bendt, F. Kraus, S. Schulz, *Angew. Chem. Int. Ed.* **2016**, *55*, 10562–10576.
- [25] BrukerAXS, *Billerica*, **2016**.
- [26] G. M. Sheldrick, *Acta Crystallogr. Sect. C* **2015**, *71*, 3–8.
- [27] G. M. Sheldrick, *Acta Crystallogr. Sect. A* **2008**, *64*, 112–122.
- [28] A. A. Coelho, in *TOPAS Academic*, 6 ed., Brisbane (Australia), **2016**.

Manuscript received: October 11, 2023

Revised manuscript received: November 22, 2023

Accepted manuscript online: November 23, 2023